

Most probable transition paths in eutrophicated lake ecosystem under Gaussian white noise and periodic force

Jinlian Jiang(姜金连), Wei Xu(徐伟), Ping Han(韩平), and Lizhi Niu(牛立志)

Citation: Chin. Phys. B, 2022, 31 (**6**): 060203. DOI: 10.1088/1674-1056/ac5616
Journal homepage: http://cpb.iphy.ac.cn; http://iopscience.iop.org/cpb

What follows is a list of articles you may be interested in

Dynamical analysis for hybrid virus infection system in switching environment

Dong-Xi Li(李东喜), Ni Zhang(张妮)
Chin. Phys. B, 2020, 29 (**9**): 090201. DOI: 10.1088/1674-1056/ab8c3f

Stochastic responses of tumor—immune system with periodic treatment

Dong-Xi Li(李东喜), Ying Li(李颖)
Chin. Phys. B, 2017, 26 (**9**): 090203. DOI: 10.1088/1674-1056/26/9/090203

Smoothing potential energy surface of proteins by hybrid coarse grained approach

Yukun Lu(卢禹锟), Xin Zhou(周昕), ZhongCan OuYang(欧阳钟灿)
Chin. Phys. B, 2017, 26 (**5**): 050202. DOI: 10.1088/1674-1056/26/5/050202

Stochastic response of van der Pol oscillator with two kinds of fractional derivatives under Gaussian white noise excitation

Yong-Ge Yang(杨勇歌), Wei Xu(徐伟), Ya-Hui Sun(孙亚辉), Xu-Dong Gu(谷旭东)
Chin. Phys. B, 2016, 25 (**2**): 020201. DOI: 10.1088/1674-1056/25/2/020201

Light trapping characteristics of glass substrate with hemisphere pit arrays in thin film Si solar cells

Chen Le, Wang Qing-Kang, Wangyang Pei-Hua, Huang Kun, Shen Xiang-Qian
Chin. Phys. B, 2015, 24 (**4**): 040202. DOI: 10.1088/1674-1056/24/4/040202

Most probable transition paths in eutrophicated lake ecosystem under Gaussian white noise and periodic force

Jinlian Jiang(姜金连), Wei Xu(徐伟)†, Ping Han(韩平), and Lizhi Niu(牛立志)

School of Mathematics and Statistics, Northwestern Polytechnical University, Xi'an 710072, *China*

(Received 5 November 2021; revised manuscript received 12 January 2022; accepted manuscript online 17 February 2022)

The effects of stochastic perturbations and periodic excitations on the eutrophicated lake ecosystem are explored. Unlike the existing work in detecting early warning signals, this paper presents the most probable transition paths to characterize the regime shifts. The most probable transition paths are obtained by minimizing the Freidlin–Wentzell (FW) action functional and Onsager–Machlup (OM) action functional, respectively. The most probable path shows the movement trend of the lake eutrophication system under noise excitation, and describes the global transition behavior of the system. Under the excitation of Gaussian noise, the results show that the stability of the eutrophic state and the oligotrophic state has different results from two perspectives of potential well and the most probable transition paths. Under the excitation of Gaussian white noise and periodic force, we find that the transition occurs near the nearest distance between the stable periodic solution and the unstable periodic solution.

Keywords: eutrophicated lake ecosystem, Freidlin–Wentzell action functional, Onsager–Machlup action functional, most probable transition path

PACS: 02.50.–r, 02.50.Fz, 02.60.Cb **DOI:** 10.1088/1674-1056/ac5616

1. Introduction

The evolution of the lake system is a natural process and may take decades to hundreds of years from the state dominated by phytoplankton to the state governed by higher aquatic plants. However, disturbances and forces from outside the ecosystem can quickly break the natural evolution process.[1] Many investigations have manifested that ecosystem sometimes experience rapid regime shifts, as shown by transition from one stable state to another. This transition will change the nature of the ecosystem, leading to the degradation of ecosystem services.[2–5] For example, eutrophication due to excessive inputs of nutrients, mainly phosphorus, is a common problem in lakes, rivers, estuaries and coastal oceans.[6] Excess phosphorus will cause the clear-water attractor of lake change to the turbid one, which comes from sewage and industrial discharges.[7,8] Lake eutrophication has proven to be a stubborn environmental problem,[9] which seriously affects the ecological balance of the lake system. In addition, it may induce important social, economic, and environmental consequences.

Eutrophicated lake ecosystems have two stable attractors for specific parameters, corresponding to the oligotrophic and eutrophic states.[8,10] The stable states are generally related to the circulation of phosphorus between sediment and water.[8] Recently, an extensive number of researches have been conducted to explore the early warning indicators, in order to predict and describe the beginning of tipping points or critical transitions. Carpenter *et al.* indicated that the increase in the variance of dynamical variables can predict the upcoming catastrophic changes in the lake eutrophication model in advance.[11] Dakos *et al.* suggested that the flickering could serve as a warning indicator which could predict the critical transition to the eutrophic state.[12,13] Ma *et al.* considered the amplitude difference, phase lag, largest Lyapunov exponent and the Shannon entropy to detect early-warning signals of the regime shifts of the lake eutrophication system. In addition, Ma *et al.* showed that it is possible to slow down the upcoming critical transition in lake eutrophication system by Gaussian white noise and periodic excitation.[14–16] Unlike the existing works in detecting the early warning signals, we study the most probable transition paths to characterize the rapid regime shifts in lake eutrophication system between the two stable states as time goes on.

For a system with multiple attractors, the random perturbation will cause the sample trajectories of the system to depart from the basin of attraction and cross the boundary of the attract basin, or even lead to the system to transfer among multiple steady states.[17–21] Generally speaking, we utilize the deterministic trajectories to characterize the deterministic system. However, it is hard to find useful information from the trajectories to analyze the dynamics of the stochastic systems. Consequently, the most probable transition paths[22] will be introduced to research the dynamics of the stochastic system. The most probable transition path has been widely applied to many scientific fields.[23–27] However, for the ecosystem, it has few documents to research the most probable transition path. In an attempt to further characterize the state transition mechanism between the oligotrophic state and the eutrophic state

†Corresponding author. E-mail: weixunpu@nwpu.edu.cn

© 2022 Chinese Physical Society and IOP Publishing Ltd

in the lake eutrophication system, we employ the most probable transition path to research the impact of the noise on the eutrophicated lake ecosystem.

Based on the above researches, it is worthy of further study on the most probable transition paths of the lake eutrophication system under the random perturbation. This paper is organized as follows. In Section 2, we introduce the lake eutrophication model with and without period force, whose deterministic structure are discussed. Furthermore, the system under white noises is provided. Next, we give two kinds of action functionals, that is, Freidlin–Wentzell (FW) and Onsager–Machlup (OM) action functionals, to obtain the most probable transition paths in Section 3. Section 4 presents the most probable transition paths for the lake eutrophication system under Gaussian white noise and periodic excitations. Finally, we summarize the above results in Section 5.

2. Lake eutrophication system

2.1. Lake eutrophication model

We firstly introduce the one-dimensional lake eutrophication model established by Carpenter *et al.*[8] The lake eutrophication model considers the phosphorus exchange between the interface of water and sediment in the lake as one of the main sources of water nutrients, and represents the level of eutrophication with the dynamic changes in the water environment of the lake. It has the following form:

$$\frac{\mathrm{d}x}{\mathrm{d}t} = \alpha - sx + r\frac{x^p}{x^p+1}, \tag{1}$$

where the dynamical variable x represents the phosphorus concentration, α represents the phosphorus input rate as control parameter, s denotes the phosphorus sink rate, r denotes the maximum rate of phosphorus recycling, and p is the Hill coefficient. As in Ref. [13], we select system parameters as $s=1$, $r=1$, and $p=8$. Then system (1) can be rewritten as

$$\frac{\mathrm{d}x}{\mathrm{d}t} = \alpha - x + \frac{x^8}{x^8+1} = f(x). \tag{2}$$

The bifurcation diagram for the parameter α is given in Fig. 1(a). Its middle-dashed line indicates the unstable equilibrium points. In the bistable region (shaded part), Eq. (2) has three equilibria under certain control parameters α. We use x_{S} to represent the unstable equilibrium point, and use x_{L} and x_{H} to represent the oligotrophic state and the eutrophic state, respectively.

Figure 1(b) shows the potentials of Eq. (2) for three different α, where $U(x) = -\int f(x)\mathrm{d}x$ represents the potential function of system (2). From the perspective of the potential well, the oligotrophic state is more stable than the eutrophic state $\alpha = 0.40$. Nevertheless, the eutrophic state is more stable than the oligotrophic state at $\alpha = 0.64$. Specially, the stability of x_{L} and x_{H} is almost the same when $\alpha = 0.52$.

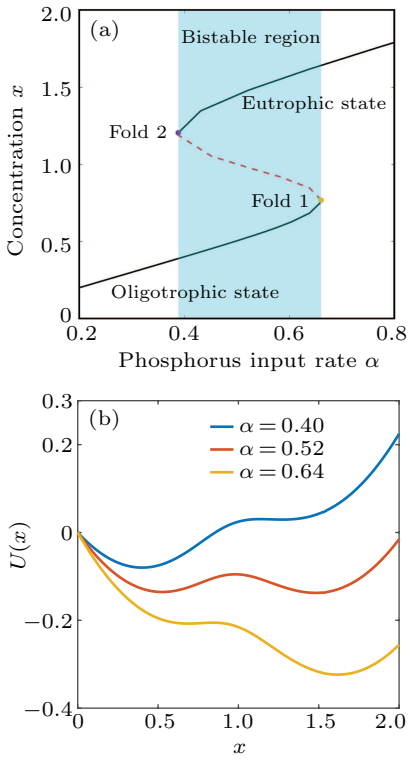


Fig. 1. (a) Bifurcation diagram for the parameter α of the system (2). The cyan shaded part defines the bistable region, where the system has three equilibria. (b) The potential of the lake eutrophication system for different α.

2.2. Lake eutrophication model with period force

The change of season, annual cycle, rainfall and so on all affect the ecosystem. And research shows that periodic force can slow down the upcoming critical transition of the lake eutrophication system.[16] The effect of the periodic excitation on the ecosystem is worthy of the further study,

$$\frac{\mathrm{d}x}{\mathrm{d}t} = \alpha - x + \frac{x^8}{x^8+1} + A\cos(\omega t) \triangleq f(x,t) \tag{3}$$

in which $A\cos(\omega t)$ represents the periodic force with the amplitude A and the frequency ω.

The time history diagram shows that nullclines $f(x,t)=0$ have different features for different A and α, in the (t,x)-plane in Fig. 2.

In Fig. 2(a), the nullines consist of three independent curves and divide the (x,t) plane into four parts, which means that $f(x,t)=0$ has three different roots at any time. And given the parameters, the system (3) has two stable periodic solutions and one unstable periodic solution. Let x_{L}^* and x_{H}^* correspond to the oligotrophic stable periodic solution and the eutrophic stable periodic solution, respectively, and x_{S}^* corresponds to the unstable periodic solution.

In Figs. 2(b) and 2(c), $f(x,t)=0$ has three different solutions at some times, and only one solution at other times. Which means the double well structure of the original system is temporarily lost during certain stages. And the number of periodic solutions is affected by parameter ω. In

Fig. 2(b), the nulline divides the (x,t) plane into two parts by a curve. In Fig. 2(c), the nullines are composed of several independent curves, among which one nulline always exists, while other closed curves only appear in certain periods.

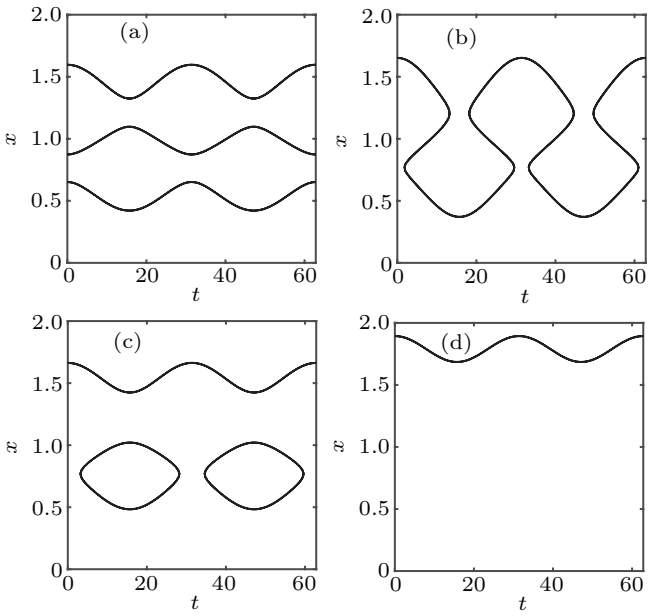


Fig. 2. The nullclines ($f(x,t)=0$) of the system (3) with $\omega=0.2$. (a) $A=0.1$, $\alpha=0.52$; (b) $A=0.15$, $\alpha=0.52$; (c) $A=0.1$, $\alpha=0.58$; (d) $A=0.1$, $\alpha=0.8$.

In Fig. 2(d), a nulline divides the (x,t) plane into two parts by a curve. In this region, $f(x,t)=0$ there is only one root at any time, and the system has only one eutrophic stable periodic solution.

2.3. Lake eutrophication system with Gaussian white

In order to describe the ecological model of lake eutrophication more accurately, the influence of environmental disturbance must be considered. Environmental disturbance has always been considered as an important factor in ecosystem modeling. On the one hand, it is the inherent uncertainty of the ecosystem. On the other hand, anthropogenic disturbances add to the uncertainty of the ecosystem.[28] In lake eutrophication system, Carpenter and Brock[29] pointed out that phosphorus input rates are affected by external fluctuations. This means that the phosphorus input rate α is a random variable. Consequently, we consider the systems (2) and (3) with Gaussian white noise

$$\frac{\mathrm{d}x}{\mathrm{d}t}=\alpha-x+\frac{x^8}{x^8+1}+\xi(t), \tag{4}$$

$$\frac{\mathrm{d}x}{\mathrm{d}t}=\alpha-x+\frac{x^8}{x^8+1}+A\cos(\omega t)+\xi(t), \tag{5}$$

where $\xi(t)$ satisfies $\langle\xi(t)\rangle=0$, $\langle\xi(t)\xi(t+\tau)\rangle=\sigma\delta(\tau)$.

With three representative potentials as shown in Fig. 2, we consider the most probable transition paths under Gaussian white noise. For system with periodic excitation, the double well structure is temporarily lost and the periodic solution is affected by parameters. Hence, we choose two groups of appropriate parameters to study the most probable paths of the periodic excitation system.

3. Two kinds of action functionals

3.1. Freidlin–Wentzell action functional

For the stochastic bistable system, noise could lead to transitions from one stable state to another stable state. If the noise intensity σ is small, the large deviation theory is a powerful method to study the noise induced transition. Freidlin and Wentzell introduced the action functional with path as the variable, which describes the probability of sample trajectory[22]

$$P\{\rho_{0T}(X^\sigma,\varphi)<\delta_0\}\approx\exp\{-\sigma^{-2}S_{0T}(\varphi)\}, \tag{6}$$

where σ represents the noise intensity, X^σ is the sample trajectory of the disturbed system, φ is the absolutely continuous function in $C_{0,T}(R^n)$, ρ represents the distance on the function space $\bar{C}[0,T]$, and $S_{0T}(\varphi)$ is the action functional. According to Eq. (6), the trajectory corresponding to the minimum of the action functional has an overwhelming probability, while the probability of other trajectories decreases exponentially. The quasi-potential has the following form:

$$S(x_1,x_2)=\inf_{T>0}\inf_{\varphi\in\bar{C}[0,T]}\{S_{0T}(\varphi)|\varphi(0)=x_1,\varphi(T)=x_2\}, \tag{7}$$

where x_1 is the starting point of the path, and x_2 is the ending point of the path. The trajectory corresponding to the quasi-potential is the most probable path of the system from the initial position x_1 to the end point x_2.

In order to obtain the most probable transition path, we use an approximate solution in WKB form when $\sigma\to0$,[30,31]

$$p(\boldsymbol{x})\sim z(\boldsymbol{x})\exp\left\{-\frac{S(\boldsymbol{x})}{\sigma}\right\}, \tag{8}$$

where $z(\boldsymbol{x})$ denotes the prefactor function that is not studied in this literature, and the FW action functional $S(\boldsymbol{x})$ represents the activation energy of fluctuations in the stochastic system. Substituting Eq. (8) into the Fokker–Planck equation leads to

$$\begin{aligned}&\sigma^{-1}\exp\left\{-\frac{S(\boldsymbol{x})}{\sigma}\right\}z(\boldsymbol{x})\left[S'(\boldsymbol{x})f(\boldsymbol{x})+\frac{1}{2}\left(S'(\boldsymbol{x})\right)^2\right]\\&-\sigma^0\exp\left\{-\frac{S(\boldsymbol{x})}{\sigma}\right\}\left[f(\boldsymbol{x})z'(\boldsymbol{x})+f'(\boldsymbol{x})z(\boldsymbol{x})\right.\\&\left.+z'(\boldsymbol{x})S'(\boldsymbol{x})+\frac{1}{2}z(\boldsymbol{x})S''(\boldsymbol{x})\right]\\&+O\left(\sigma\exp\left\{-\frac{S(\boldsymbol{x})}{\sigma}\right\}\right)=0.\end{aligned} \tag{9}$$

And keeping only the terms of lowest order in σ, we acquire the Hamilton–Jacobi equation for $S(\boldsymbol{x})$

$$H(\boldsymbol{x},\boldsymbol{p})=b(\boldsymbol{x})\boldsymbol{p}+\frac{1}{2}\boldsymbol{p}^{\mathrm{T}}\boldsymbol{p}=0,$$

$$\boldsymbol{p}=\frac{\partial S}{\partial \boldsymbol{x}}, \tag{10}$$

where $\boldsymbol{p}$ stands for momentum. In order to solve Eq. (10), we utilize the method of characteristics[32] to derive the following equations:

$$\begin{aligned}\dot{\boldsymbol{x}}&=\frac{\partial H}{\partial \boldsymbol{p}}=b(\boldsymbol{x})+\boldsymbol{p},\\ \dot{\boldsymbol{p}}&=\frac{\partial H}{\partial \boldsymbol{x}}=-\left[\frac{\partial b(\boldsymbol{x})}{\partial \boldsymbol{x}}\right]^{\mathrm{T}}\boldsymbol{p},\end{aligned} \tag{11}$$

and the evolution equation of S along the characteristic line

$$\frac{\mathrm{d}S}{\mathrm{d}t}=\boldsymbol{p}\dot{\boldsymbol{x}}. \tag{12}$$

Equation (11) is an auxiliary Hamiltonian system,[33] and $\boldsymbol{p}$ represents the disturbance term in the original equation. Thus, the most probable transition path can be obtained from Eq. (11). If the original fixed point is a stable equilibrium point, the noise disturbance can add an unstable manifold; if the original fixed point is an unstable equilibrium point, the noise disturbance can lead to a stable manifold. We apply the action plot to get the FW action functionals of the escape paths. From this we can acquire the minimum of the FW action functional and the corresponding most probable transition path.

3.2. Onsager–Machlup action functional

The noise intensity also has an important effect on lake eutrophication system, so it is worthy to further discuss the most probable transition paths under different noise intensities. We obtain the most probable transition path by minimizing the OM action functional[34–36] for the stochastic lake eutrophication systems (4) and (5). According to the principle of least action principle, the most probable transition path x_{m} can be obtained by

$$\delta\int_0^T OM\left(\dot{x},x\right)\mathrm{d}t=0, \tag{13}$$

where the integral $\int_0^T OM\left(\dot{x},x\right)\mathrm{d}t$ is the OM action functional, and δ stands for the functional differentiation defined as

$$\frac{\delta F}{\delta f(x)}=\lim_{\varepsilon\to 0}\frac{F\left[f(x)+\varepsilon\delta\left(x-x'\right)\right]-F\left[f(x)\right]}{\varepsilon}. \tag{14}$$

According to Eq. (13), it can be deduced that OM functional satisfies the Euler–Lagrange equation

$$\frac{\mathrm{d}}{\mathrm{d}t}\frac{\partial OM\left(\dot{x},x\right)}{\partial\dot{x}}=\frac{\partial OM\left(\dot{x},x\right)}{\partial x}, \tag{15}$$

where the OM function $OM\left(\dot{x},x\right)$ of system (4) is defined by

$$OM\left(\dot{x},x\right)=\left(\frac{f(x)-\dot{x}}{\sigma}\right)^2+f'(x). \tag{16}$$

Therefore, the most probable transition path $x_{\mathrm{m}}(t)$ satisfies the following equation:

$$\begin{cases}\ddot{x}_{\mathrm{m}}(t)=\dfrac{\sigma^2}{2}f''(x_{\mathrm{m}})+f'(x_{\mathrm{m}})f(x_{\mathrm{m}}),\\ x_{\mathrm{m}}(0)=x_{\mathrm{L}},\quad x_{\mathrm{m}}(T)=x_{\mathrm{H}},\end{cases} \tag{17}$$

where σ represents noise intensity, x_{L} is the initial value of the most probable paths, x_{H} is the final value of the most probable path, and T is the total time. By solving Eq. (17), the most probable paths of system (4) under different noise intensities can be obtained.

For the stochastic system (5), $x_{\mathrm{m}}(t)$ satisfies the following equation:[37]

$$\begin{cases}\ddot{x}_{\mathrm{m}}(t)=\dfrac{\sigma^2}{2}f_{xx}\left(x_{\mathrm{m}},t\right)+f_x\left(x_{\mathrm{m}},t\right)f\left(x_{\mathrm{m}},t\right)+f_t\left(x_{\mathrm{m}},t\right),\\ x_{\mathrm{m}}(0)=x_{\mathrm{L}}^*(0),\quad x_{\mathrm{m}}(T)=x_{\mathrm{H}}^*(\mathrm{T}),\end{cases} \tag{18}$$

where σ represents noise intensity, $x_{\mathrm{L}}^*(0)$ is a point on the periodic solution, x_{L}^* is the initial value of the most probable paths, $x_{\mathrm{H}}^*(0)$ is a point on the periodic solution, x_{H}^* as the final value of the most probable path, and T is the total time. By solving Eq. (18), the most probable paths of system (5) under different noise intensities can be obtained.

4. Results

In this section, we use the above two methods to compute the most probable transition paths. The characteristics of the most probable transition path can help analyze how the lake transfers between the oligotrophic state and the eutrophic state. For stochastic systems, we utilize FW action functional to get the most probable transition paths in weak noise. In addition, we use the OM action functional to study the influence of the noise intensity on the most probable transition path.

4.1. Lake eutrophication system under Gaussian white noise

For system (4), we display the most probable transition paths between x_{L} and x_{H} for different α. According to the FW large deviation theory, we acquire the most probable transition paths and the momentum required to transition from x_{L} to x_{H} with different parameters. Furthermore, by minimizing OM functional, the most probable transition paths between x_{L} and x_{H} under different noise intensity can be obtained.

As can be seen from Fig. 3, the changes of the most probable path and momentum have same characteristics. The most probable transition paths start at the stable equilibrium point x_{L}, and it wanders in the basins of x_{L} and the momentum p starts at zero and grows slowly. As time goes on, the momentum p suddenly increases and the large momentum makes the system transition from x_{L} to x_{S}. Then the momentum p rapidly decreases to zero, while the system stays at x_{S} (unstable state) for a long time. But because of the attraction of x_{H}, the system will eventually reach x_{H}.

Under different parametersα, the relative stability between the attractors is different, and the maximum momentum required for transition are different. The value of the Y-axis on the right of Fig. 3 represents the momentum of the system. The larger momentum p is, the more energy is needed to escape from the stable equilibrium point. By comparing Figs. 3(a)–3(c), it can be seen that the maximum momentum decreases successively, indicating that within a certain range, with the increase of parameter α, the lake system is easier to transition from the oligotrophic state to the eutrophic state.

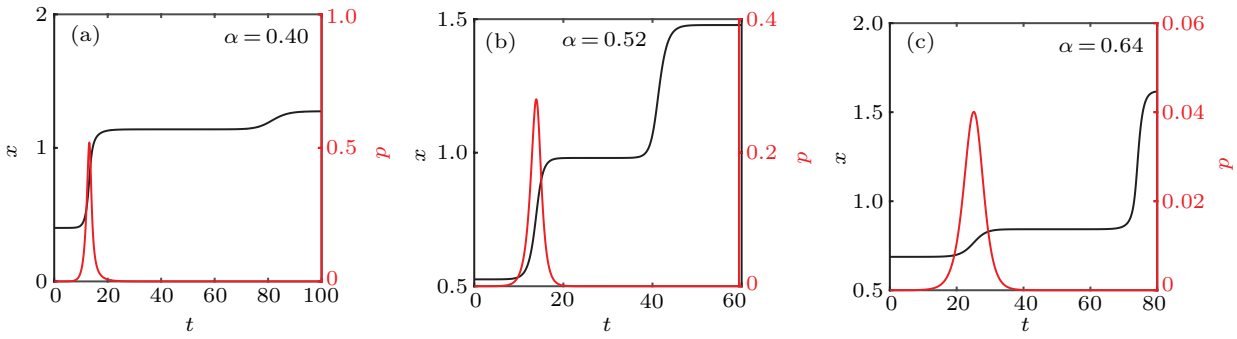


Fig. 3. The most probable paths and momentum of lake eutrophication system from x_{L} to x_{H} under different parameters α. The black lines represent the most probable escape paths, and the red lines represents the momentum change during transition. (a) $\alpha = 0.40$; (b) $\alpha = 0.52$; (c) $\alpha = 0.64$.

In Fig. 4, it is easy to understand that the most probable transition path is a heteroclinic orbit connecting three fixed points. Heterotonic orbitals visually show that the momentum p changes the topology of the original system. The most probable paths connect the three equilibrium points of the system, but not just along the x-axis. Because of the influence of p, the system transition occurs. The most probable path of the system from x_{L} to x_{S} is an arc orbit containing the manifold of the auxiliary Hamiltonian system. Once the system reaches x_{S}, the disturbance force p becomes zero and the system will relax to another equilibrium point. With the increase of parameter α, the heteroclinic orbitals from x_{L} to x_{H} are shrinking, while the heteroclinic orbitals from x_{H} to x_{L} are increasing. With the increase of parameter α, the lake system transition from the oligotrophic state to the eutrophic state requiring less energy. The results of Fig. 4 confirm the conclusion of Fig. 3.

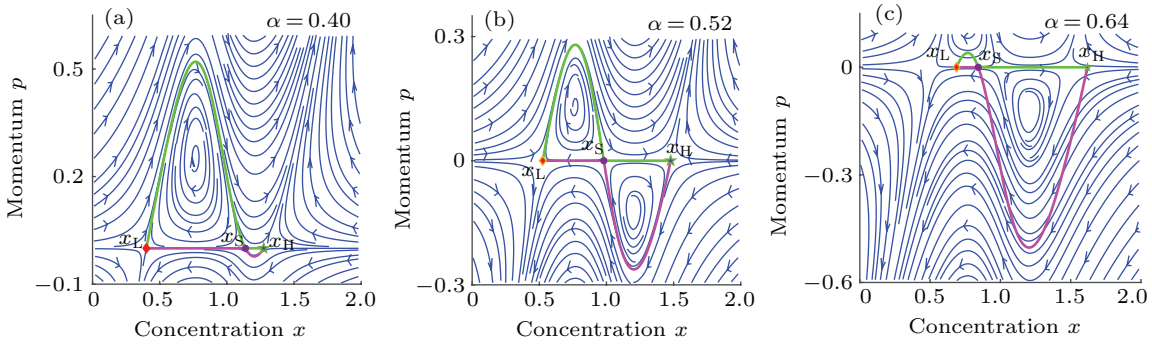


Fig. 4. Phase portrait of the Hamilton equation. The green and magenta curves represent the most probable paths from x_{L} to x_{H} and from x_{H} to x_{L}, respectively. (a) $\alpha = 0.40$; (b) $\alpha = 0.52$; (c) $\alpha = 0.64$.

In Fig. 5, we obtain the most probable transition paths $x_{\mathrm{m}}(t)$ beginning at the oligotrophic state x_{L} and ending at the eutrophic state x_{H} with different noise intensities. On the whole, the residence time of the system in oligotrophic state became shorter with the increase of parameter α. And with the increase of noise intensity, the transition time occurs earlier and the residence time in the unstable equilibrium x_{S} becomes shorter.

The inset diagrams of Figs. 5(a) and 5(b) show that the most probable paths transition between the two stable equilibrium states. When $\alpha = 0.40$, although the potential well in the eutrophic state is not deep, the system will still stay in the eutrophic state for some time. When $\alpha = 0.52$, the system will wander in the eutrophic state for a longer time. Although the difference between the depths of potential well is not great, the eutrophic state is more stable than the oligotrophic state from the perspective of the transition path. That is, eutrophication is a very difficult problem to solve. When $\alpha = 0.64$, the system switches from the oligotrophic state x_{L} to the eutrophic state x_{H} quickly, because eutrophic state is more stable at this parameter.

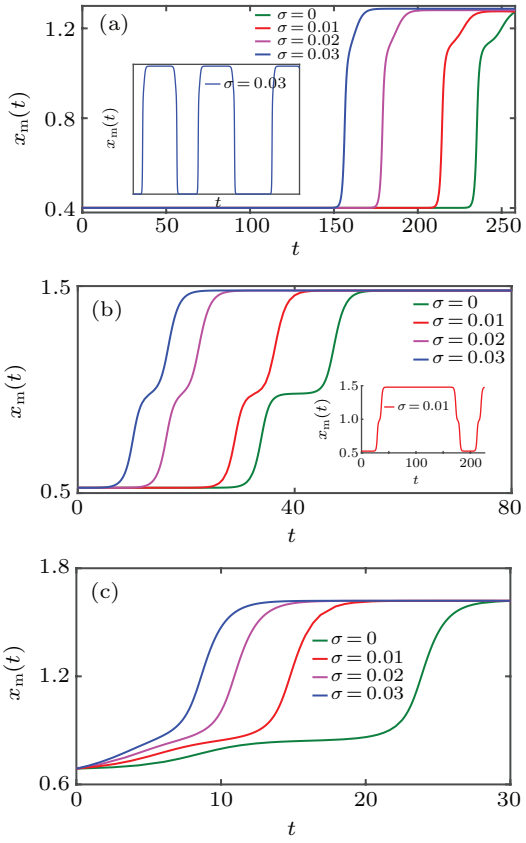


Fig. 5. Most probable transition paths $x_{\rm m}(t)$ starting at the oligotrophic state $x_{\rm L}$ and ending at the eutrophic state $x_{\rm H}$ for different noise intensities. (a) $\alpha=0.40$, the inset figure displays the most probable path between $x_{\rm L}$ and $x_{\rm H}$ at $\sigma=0.03$. (b) $\alpha=0.52$, the inset figure displays the most probable path between $x_{\rm L}$ and $x_{\rm H}$ at $\sigma=0.01$. (c) $\alpha=0.64$.

4.2. Lake eutrophication system under Gaussian white noise and periodic excitations

Now, we consider not only white Gaussian noise but also periodic excitation on the most probable transition path between the oligotrophic state and the eutrophic state. Based on the characteristic of the nullines of the periodic system, the most probable paths of the system with two sets of parameters are considered in this paper.

According to Subsection 3.1, we have the Hamiltonian for Eq. (4) as follows:

$$H(\boldsymbol{x},\boldsymbol{p}) = \left(\alpha - x + \frac{x^8}{1+x^8} + A\cos(\omega\theta)\right)p_2 + p_1 + \frac{1}{2}p_2^2, \tag{19}$$

and the auxiliary Hamiltonian system

$$\begin{aligned}
&\dot{x} = \alpha - x + \frac{x^8}{1+x^8} + A\cos(\omega\theta) + p_2,\\
&\dot{\theta} = 1,\\
&\dot{p}_1 = A\omega\sin(\omega\theta)p_2,\\
&\dot{p}_2 = \left(1 + \frac{8x^7}{(1+x^8)^2}\right)p_2.
\end{aligned} \tag{20}$$

We choose $(x,\theta) = (x_{\rm L}^*(\theta)+\delta, \theta(t))$ as the initial values, where $x_{\rm L}^*(\theta)$ are the coordinates of the stable period solution, $\theta(t)$ can help us parameterize the escape paths, ranging from $[0, 20\pi)$, and δ is a small displacement.

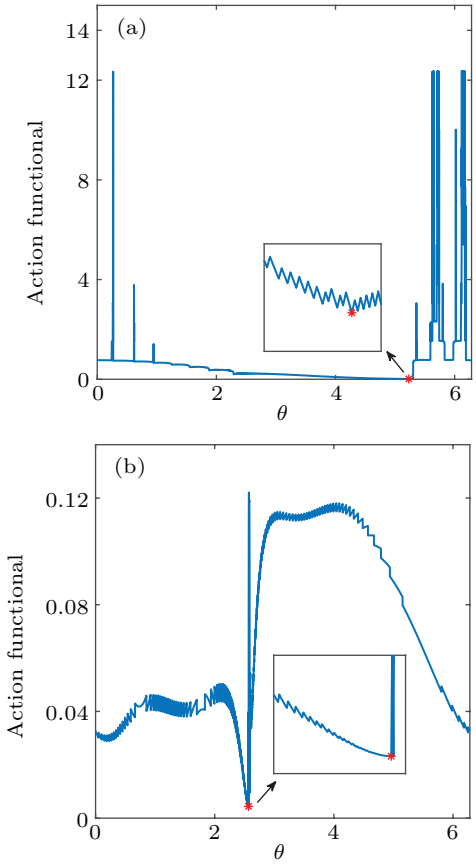


Fig. 6. Freidlin–Wentzell action functionals of escape paths from $x_{\rm L}^*$ to $x_{\rm H}^*$. The minimum of Freidlin–Wentzell action functional is marked by the red asterisk. (a) $\alpha=0.52$, $A=0.1$, $\omega=0.1$; (b) $\alpha=0.58$, $A=0.1$, $\omega=0.5$.

Figure 6 shows the action functional for different (x,θ). Its global minimum, indicated by a red asterisk, corresponds to the most probable path of the system.

In Fig. 7, the thick solid red line represents the most probable escape path. It can be seen that the transition of the most probable path occurs at the closest distance between $x_{\rm L}^*$ and $x_{\rm S}^*$. And the most probable path to $x_{\rm H}^*$ is near the intersection of the nulline and periodic solution.

For Fig. 7(a), the most probable path does not move along the unstable periodic solution after exiting from $x_{\rm L}^*$ to $x_{\rm H}^*$, but directly reaches $x_{\rm H}^*$. As can be seen from other escape paths, they firstly move towards the unstable periodic solution $x_{\rm S}^*$ but their momenta are too small to escape. Then they will fluctuate between the original stable periodic solution and the unstable periodic solution to prepare for a next trial to escape. For Fig. 7(b), after the most probable path switches from $x_{\rm L}^*$ to $x_{\rm S}^*$, it moves along the unstable periodic solution $x_{\rm S}^*$, and the most probable path begins to transition to $x_{\rm H}^*$ near the intersection of the unstable periodic solution and the nulline.

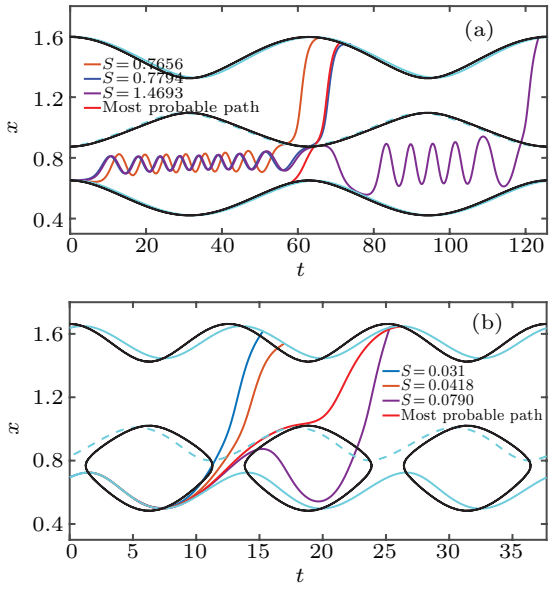


Fig. 7. Escape paths from $x_{\rm L}^*$ to $x_{\rm H}^*$. The solid cyan lines represent the two stable periodic solutions and the dotted cyan line represents the unstable periodic solutions. The black lines represent the nullclines. The red thick line represents most probable transition path, and the other lines for other escape paths. (a) $\alpha = 0.52$, $A = 0.1$, $\omega = 0.1$; (b) $\alpha = 0.58$, $A = 0.1$, $\omega = 0.5$.

In Fig. 8, we compare the most probable transition paths obtained from Eq. (19) for various values of σ. Herein, for all the most probable transition paths, we choose the same start point $x_{\rm L}^*(0)$, the same end point $x_{\rm H}^*(T)$ and the total time for five periods. Given the parameters, the nullines are very close to the periodic solutions but they do not overlap. The nullines only intersect the highest and lowest points of the periodic solutions. The insets in Fig. 8 indicate that the transition occurs in the gap between the stable periodic solution and nullcline, where the flow of the period solutions will change directions.

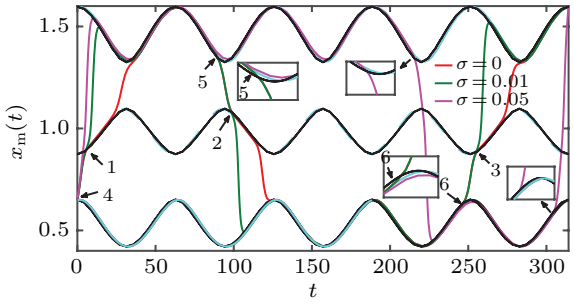


Fig. 8. Most probable transition paths for different σ with $\alpha = 0.52$, $A = 0.1$, $\omega = 0.1$. The solid cyan lines represent the two stable periodic solutions and the dotted cyan line represents the unstable periodic solution, the black lines represent the nullclines. The arrow-1 to arrow-3 mark where paths arrive at $x_{\rm S}^*$, and the arrow-4 to arrow-6 mark where paths leave $x_{\rm L}^*$ and $x_{\rm H}^*$. And the insets indicate that the transition occurs in the gap between the stable periodic solution and the nullcline.

We observe that the transition of the system occurs between two stable periodic solutions three times in five periods. The first transition is from $x_{\rm L}^*$ to $x_{\rm H}^*$, and the places leaving $x_{\rm L}^*$ and reaching $x_{\rm S}^*$ are not different with the change of noise intensity. The second transition is from $x_{\rm H}^*$ to $x_{\rm L}^*$. The residence time in $x_{\rm L}^*$ and $x_{\rm H}^*$ varies greatly under different noise intensities. When $\sigma = 0.05$, the most probable path stays longer in $x_{\rm H}^*$, while for $\sigma = 0$ and $\sigma = 0.01$, the most probable paths stay longer in $x_{\rm L}^*$. The third transition is from $x_{\rm L}^*$ to $x_{\rm H}^*$. Every transition indicates that the transition occurs near the nearest distance between the stable periodic solution and the unstable periodic solution.

When $\sigma = 0$, the most probable transition path moves along $x_{\rm S}^*$ for a half cycle after reaching the unstable periodic solution. Nevertheless, the most probable transition paths switch quickly to the other stable period solution for $\sigma = 0.01$ and $\sigma = 0.05$. And there have interesting phenomenon for $\sigma = 0$ and $\sigma = 0.01$. For each transition, the most probable transition paths follow a similar trajectory to the unstable periodic solution $x_{\rm S}^*$, marked by arrow-1 to arrow-3. And the transitions begin at a similar point at stable periodic solutions, that is, they all leave the stable periodic solution $x_{\rm L}^*$ and $x_{\rm H}^*$ around the same phase, marked by arrow-4 to arrow-6.

In Fig. 9, we compare the most probable transition paths obtained from Eq. (15) for various values of σ. Herein, for all the most probable transition paths, we choose the same start point $x_{\rm L}^*(0)$, the same end point $x_{\rm H}^*(T)$ and the total time for four periods.

As shown in Fig. 9, the influence of noise intensity on the most probable paths is not very large. Basically, the most probable paths move along $x_{\rm L}^*$ to the red square and transition to $x_{\rm H}^*$. The place where the most probable paths transition is the same, and the higher the noise intensity, the earlier the system reaches $x_{\rm H}^*$. When $\sigma = 0$, the most probable transition path moves along $x_{\rm S}^*$ for a half cycle, while when $\sigma \neq 0$, the most probable paths hardly stay at $x_{\rm S}^*$.

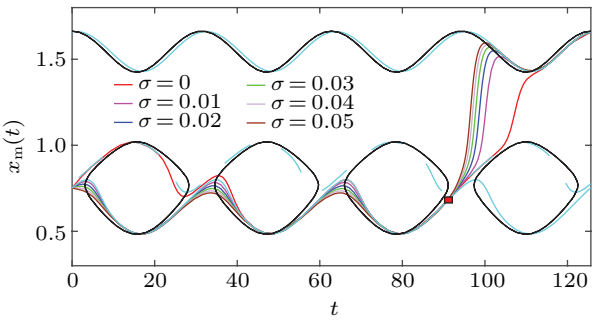


Fig. 9. Most probable transition paths for different σ with $\alpha = 0.58$, $A = 0.1$, $\omega = 0.5$. The solid cyan lines represent the two stable periodic solutions and the dotted cyan line represents the unstable periodic solution, the black lines represent the nullclines. The red square indicates the most probable paths transition occurs at the same place under different noise intensity.

The most probable paths will deviate from $x_{\rm L}^*$ where the double-well structure disappears. In particular, where the double-well structure of the system disappears, the most probable path at $\sigma = 0$ initially moves up to $x_{\rm S}^*$ and along it. After the unstable periodic solution intersects the nulline, the system begins to move down to $x_{\rm L}^*$ under the action of the deterministic vector field. It can be seen that when the double-well

structure disappears, the distance between x_{L}^{*} and x_{S}^{*} is closest, and the system is prone to transition.

5. Conclusions

In this paper, we have investigated the most probable transition paths of the lake eutrophication system under Gaussian white noise and the periodic force. The characterization of the most probable paths provides a new perspective for the study of the lake eutrophication system. We visualized transitions between the eutrophic state and the oligotrophic state. We introduced two kinds of action functionals, FW action functional and OM action functional, for the calculation of the most probable transition paths under different noise intensities.

Firstly, the influence of noise is only considered. We used large deviation theory to observe the most probable transition paths. In weak noise intensity, the Hamilton–Jacobi equation is obtained by using WKB approximation for the system, and the FW action functional is obtained by using the method of characteristics. We used the minimum of the FW action functional to obtain the most probable transition paths between the oligotrophic state the eutrophic state. Further, we examined the most probable transition paths $x_{\mathrm{m}}(t)$ from the oligotrophic state x_{L} to the eutrophic state x_{H} with different noise intensities by minimizing the OM action functional. By characterizing the most probable transition paths under certain parameters, we have found that the stability of the eutrophic state and the oligotrophic state has different results from the two perspectives of potential well and the most probable transition path.

Then, Gaussian white noise and periodic excitation were considered. Considering the influence of parameters on the periodic solutions and nullines of the system, we have chosen two groups of parameters to study the most probable path of the system with periodic excitation. The most probable transition paths from x_{L}^{*} to x_{H}^{*} were obtained by using the large deviation theory. In addition, by minimizing the OM functional, we obtained the most probable transition paths starting at the same initial point on x_{L}^{*} and terminating on x_{H}^{*} for different noise intensities. The transition points in periodic lake eutrophication system have same characteristics, and the transition is more likely to occur near the closest distance between stable and unstable periodic solutions.

Acknowledgement

Projected supported by the National Natural Science Foundation of China (Grant Nos. 12072261 and 11872305).

References

[1] Burkett V R, Wilcox D A, Stottlemyer R, Barrow W, Fagre D, Baron J, Price J, Nielsen J L, Allen C D, Peterson D L, Ruggerone G and Doyle T 2005 *Ecolog. Complex.* **2** 357
[2] Scheffer M, Carpenter S, Foley J A, Folke C and Walker B 2001 *Nature* **413** 591
[3] Zhang H, Xu W, Han P and Qiao Y 2020 *Phys. A* **556** 124809
[4] Zhang H, Xu W, Guo Q, Han P and Qiao Y 2020 *Chaos Solitons Fract.* **135** 109767
[5] Zhang H, Xu W, Lei Y and Qiao Y 2019 *Commun. Nonlinear Sci. Numer. Simulat.* **77** 258
[6] Schindler D W 1977 *Science* **195** 260
[7] Carpenter S R 2005 *Proc. Natl. Acad. Sci. USA* **102** 10002
[8] Carpenter S R, Ludwig D and Brock W A 1999 *Ecolog. Appl.* **9** 751
[9] Carpenter S R, Caraco N F, Correll D L, Howarth R W, Sharpley A N and Smith V H 1998 *Ecolog. Appl.* **8** 559
[10] Scheffer M, Brock W and Westley F 2000 *Ecosystems* **3** 451
[11] Carpenter S and Brock W 2006 *Ecology Lett.* **9** 311
[12] Dakos V, van Nes E H and Scheffer M 2013 *Theoret. Ecology* **6** 309
[13] Wang R, Dearing J A, Langdon P G, Zhang E, Yang X, Dakos V and Scheffer M 2012 *Nature* **492** 419
[14] Ma J, Xu Y, Kurths J, Wang H and Xu W 2018 *Chaos* **28** 113601
[15] Ma J, Xu Y, Li Y, Tian R and Kurths J 2019 *Chaos* **29** 081102
[16] Ma J, Xu Y, Xu W, Li Y and Kurths J 2019 *Sci. China-Techn. Sci.* **62** 2144
[17] Li P, Nie L R, Huang Q R and Sun X X 2012 *Chin. Phys. B* **21** 050503
[18] Ruyin C, Wanli P, Jianqiang Z and Linru N 2016 *Chaos* **26** 093113
[19] Jianqiang Z, Linru N, Chongyang C and Xinyu Z 2016 *AIP Advances* **6** 075212
[20] Chen R, Chen C and Nie L 2017 *Int. J. Mod. Phys. B* **31** 1750259
[21] Chen R, Pan L, Nie L, Chen C, Zeng C and Liu S 2019 *Indian J. Phys.* **93** 115
[22] I Freidlin M and D Wentzell A *Random Perturbations of Dynamical Systems* (Berlin, Heidelberg: Springer) p. 2012
[23] Chen H, Shen C, Zhang H and Kurths J 2017 *Chaos* **27** 081102
[24] Chen X, Wu F, Duan J, Kurths J and Li X 2019 *Appl. Math. Comput.* **348** 425
[25] Franovic I, Todorovic K, Perc M, Vasovic N and Buric N 2015 *Phys. Rev. E* **92** 062911
[26] Tsiairis A, Wei P, Chao Y and Duan J 2021 *Phys. A* **569** 125749
[27] Wells D K, Kath W L and Motter A E 2015 *Phys. Rev. X* **5** 031036
[28] Folke C, Carpenter S, Walker B, Scheffer M, Elmqvist T, Gunderson L and Holling C S 2004 *Annual Review of Ecology, Evolution, and Systematics* **35** 557
[29] Brock W and Carpenter S 2006 *Ecology and Society* **11** 9
[30] Luchinsky D G and McClintock P V E 1997 *Nature* **389** 463
[31] Maier R S and Stein D L 1996 *J. Statist. Phys.* **83** 291
[32] Ludwig D 1975 *Siam Review* **17** 605
[33] Beri S, Mannella R, Luchinsky D G, Silchenko A N and McClintock P V E 2005 *Phys. Rev. E* **72** 036131
[34] Durr D and Bach A 1978 *Commun. Math. Phys.* **60** 153
[35] Onsager L and Machlup S 1953 *Phys. Rev.* **91** 1505
[36] Tisza L and Manning I 1957 *Phys. Rev.* **105** 1695
[37] Chen Y, Gemmer J A, Silber M and Volkening A 2019 *Chaos* **29** 043119